Utility of a New Bolus-Injectable Nanoparticle for Clinical Cancer Staging[1]

Mukesh Harisinghani[*,†], *Robert W. Ross*[*,†], *Alexander R. Guimaraes*[*,†] *and Ralph Weissleder*[*,†,‡]

*Center for Molecular Imaging Research, Massachusetts General Hospital, Boston, MA, USA; †Harvard Cancer Center, Boston, MA, USA; ‡Center for Systems Biology, Massachusetts General Hospital, Boston, MA, USA

Abstract

BACKGROUND: In this study, we report on the use of a new, bolus-injectable, carboxymethyl dextran–based magnetic nanoparticle (MNP), ferumoxytol, to improve detection in loco-regional lymph nodes by magnetic resonance imaging (MRI). METHODS: This preliminary study was performed as a prospective, single-center, open label pilot study to determine the magnitude of nodal MRI signal changes and to determine the optimal time points for imaging following intravenous (IV) bolus injection of the MNP. The study group consisted of 10 patients, all of whom were diagnosed with prostate cancer before any systemic therapy. RESULTS: All 10 patients had lymph nodes evaluated by histopathology. Of the evaluated 26 lymph nodes, 20 were benign and 6 were malignant. The mean short-axis diameter of benign lymph nodes was 6 mm and the mean short-axis diameter of malignant lymph nodes was 7 mm. Following IV administration, there was a significant change in mean signal-to-noise ratio (SNR) of benign lymph nodes ($P < .0001$) whereas there was little change in the mean SNR of malignant nodes ($P = .1624$). No adverse events were encountered. CONCLUSION: Ferumoxytol is safe and, at the appropriate circulation interval, modulates nodal signal intensity, allowing for identification of malignant nodal involvement by MRI.
Neoplasia (2007) **9,** 1160–1165

Introduction

Nanotechnology has been hailed as an enabling science, leading to new drugs, products, sensors, and devices, and has been most successful in the preclinical area [1]. Despite numerous advances, including a National Nanotechnology Initiative [2,3], clinical translation has been slow. In fact, to date, the most successful clinical nanomaterials have been diagnostic imaging agents [1]. Based on anecdotal studies that certain nanomaterials (e.g., tantalum and thorium dioxide nanoparticles) have a propensity for accumulating in nodal macrophages, we designed biocompatible and magnetic resonance imaging (MRI)–detectable analogs nearly two decades ago [4]. These materials (originally dubbed ultrasmall superparamagnetic iron oxide [USPIO] and later

monocrystalline iron oxide nanocolloid [MION]) were dextran T10–coated superparamagnetic nanoparticles in the 20- to 50-nm size range, with variable coating thickness to impart distinct pharmacokinetic properties and macrophage recognition through opsonization and/or protein binding. We subsequently conducted clinical trials on one prototype, ferumoxtran-10 (Combidex; AMAG Pharmaceuticals Inc., Cambridge, MA), as the first systemically injectable lymphotropic imaging agent [5,6]. In subsequent larger-scale trials, we and others were able to demonstrate extraordinary efficacy of this material [7–10]. However, despite this proven efficacy, ferumoxtran-10 has some logistical disadvantages, including the need for a slow infusion to minimize hypersensitivity-related side effects.

In an effort to produce nanomaterials with improved surface coatings, higher iron payloads and ability for bolus injection, carboxymethyl dextran (polyglucose sorbitol carboxymethylether) nanoparticles have been developed as next-generation nanoparticles. One such clinical prototype preparation, ferumoxytol (Code 7228; AMAG Pharmaceuticals Inc.), is being developed for iron replacement therapy in anemia [11–13]. The safety profile of ferumoxytol in phase I and II clinical trials has been very good (better than oral elemental iron), enabling the administration at substantially higher doses compared to ferumoxtran^{-10}. In the anemia setting, 1000 mg Fe of nanoparticles is administered intravenously (IV) in two settings, roughly four times the diagnostic dose of the earlier ferumoxtran^{-10} (2.6 mg Fe/kg). Ferumoxytol also has a shorter blood half-life in humans (10–14 hours) and greater T1 shortening of blood (increased signal of blood vessels) leading to its past exploration as a vascular imaging agent for MRI [12]. It has remained unclear, however, whether the therapeutic agent ferumoxytol can be used as a diagnostic lymphotropic imaging agent given its different effects on tissue relaxation times. In particular, the dose and the time to image after magnetic nanoparticle (MNP) administration to achieve maximal contrast within human lymph

nodes remain unknown. The purpose of this exploratory study was to test this bolus-injectable MNP in patients with prostate cancer with possible nodal spread, to document changes in nodal signal intensities as a function of time (serial imaging), and to document side effects upon bolus injection.

Materials and Methods

This exploratory study, sponsored by the National Cancer Institute, was performed as a prospective, single-center, single-dose, open label pilot study and was approved by the Institutional Review Board.

Subjects

Subjects with prostate cancer who were scheduled for a surgical lymph node dissection were eligible for this study. Other entry criteria included the following: age > 18 years; no prior therapy for metastatic disease; no evidence of iron overload; and normal liver function tests. Subjects with a known iron allergy were also excluded.

Study Procedures

Nanoparticle   Ferumoxytol (AMAG Pharmaceuticals Inc.) is a superparamagnetic iron oxide nanoparticle designed to minimize immunologic sensitivity. The crystal size of the iron oxide core is 6.8 ± 0.4 nm in diameter as measured by X-ray diffraction [12]. The nanoparticle is formulated to be isotonic at a concentration of 30 mg Fe/ml. The physical, pharmacokinetic, and biologic properties of ferumoxytol in therapeutic trials have been reported [11,12]. Ferumoxytol was administered at a dose of 4 mg of Fe/kg, injected at a rate of 2 ml/sec by using a power injector (Medrad Spectris; Medrad, Indianola, PA). A 15-ml normal saline intravenous flush was given after the nanoparticle administration. Vital signs were monitored throughout the entire study and 2 hours after termination of imaging.

Patients   The study group consisted of 10 patients (mean age 53.8 years; range 43−70 years), all of whom were diagnosed with prostate cancer before any systemic therapy. Patient characteristics are summarized in Table 1.

The patients were screened for known allergy or hypersensitivity reactions to parenteral iron, parenteral dextran, parenteral iron−dextran, or parenteral iron−polysaccharide preparations and, if present, were excluded from the study. Similarly, any pre-study documented ferritin level in the

available medical records greater than 800 ng/ml and percent saturation of transferrin level greater than 60% or any laboratory/clinically confirmed history of iron overload or hemachromatosis resulted in exclusion from the study.

MR imaging   MR imaging of the pelvis was performed on a 1.5-T scanner (Signa; General Electric Medical Systems, Milwaukee, WI) using a pelvic phased array coil. T1-, T2-, and T2*-weighted imaging was performed from the pubic symphysis to the aortic bifurcation in the axial and coronal plane using the following parameters: 1) T2-weighted fast spin-echo: repetition time 4500 to 5500 msec, echo time 80 to 100 msec, flip angle 90°, number of excitations 3, slice thickness 3 mm, gap 0, matrix 256×256, field of view 22 to 30 cm; and 2) T2*-weighted gradient-echo: repetition time 2100 msec, echo time 21 msec, flip angle 20°, number of excitations 2, slice thickness 3 mm, gap 0, matrix 160×256, field of view 22 to 30 cm. Imaging was performed before, and at 5, 18, and 24 hours following the intravenous administration of ferumoxytol. Imaging times ranged from 30 to 45 minutes. All patients were imaged with the same sequence parameters.

Follow-up   All patients were followed up for adverse events. The patient's vital signs including pulse oximetry, heart rate, and blood pressure were recorded just before the ferumoxytol infusion, every 5 minutes for 30 minutes following the ferumoxytol bolus and every 30 minutes following the ferumoxytol injection for a minimum of 2 hours. The patients were monitored for adverse events for 2 hours after the infusion and at every patient visit thereafter. At every subsequent MRI time point, the vitals were repeated and patients were again evaluated for adverse events at each contact time. The pathologic outcomes from their lymph node dissection were recorded. Patients were followed up for 2 weeks following the termination of the entire study to determine any possible side effects from ferumoxytol administration.

Image Analysis

Signal-to-noise ratios (SNRs) of muscle, fat, bone marrow, and lymph nodes were determined on T2*-weighted images by placing operator-defined region-of-interest. SNR was determined by dividing the mean signal intensity of a lymph node by the standard deviation of background noise. The paired Student's *t* test was used to evaluate the statistical significance between benign and malignant lymph nodes at different time points.

Table 1. Characteristics of Patients Enrolled in the Study.

Patient	Age (years)	PSA (ng/ml)	Gleason Score	Clinical T Stage
1	55	20.3	6	T1c
2	46	4.4	7	T2c
3	44	7.07	6	T1c
4	58	27	9	T2
5	70	16.8	7	T1c
6	51	4.6	9	T1c
7	62	6	9	T2b
8	60	7.4	7	T2a
9	43	0.1	6	T2
10	49	2.6	6	T2a

Results

All patients completed the study and no adverse events were noted during nanoparticle injection or within 2 weeks of follow-up. Of the 10 patients, 4 also had surgical nodal dissection of lymph nodes [benign ($n = 3$); malignant ($n = 1$)] and 6 had image-guided lymph node biopsy [benign ($n = 4$); malignant ($n = 2$)]. The mean size of the biopsied lymph nodes was 8 mm (range 7−11 mm). A total of 26 lymph nodes were then evaluated histopathologically. Of these, 20 were benign and 6 were malignant. The mean short-axis

diameter of benign lymph nodes was 6 mm and the mean short-axis diameter of malignant lymph nodes was 7 mm.

Effect of the Nanoparticle on Normal Tissues

Figure 1 summarizes the SNR of different tissues (muscle, fat, bone marrow, and lymph node) for different patients as a function of IV administration of ferumoxytol. In muscle and fat, SNR did not change appreciably ($P > .5$), whereas that of bone marrow decreased slightly. In contradistinction, SNR of benign lymph nodes decreased in all patients.

Effect of the Nanoparticle on Malignant Lymph Nodes

Figure 2*A* compares MR signal intensities in normal and metastatic lymph nodes on a group by group basis. As expected, benign and malignant nodes had similar SNR before administration of nanoparticle ($P = .27$). Following IV administration, there was a significant change in mean SNR of benign lymph nodes (9.26 ± 2.11 to 2.94 ± 1.34, representing a 68.2% change; $P < .0001$). In contradistinction, there was little change in the SNR of malignant nodes (7.46 ± 1.83 to 6.83 ± 1.35, representing an 8.5% change; $P = .1624$). Figure 2*B* plots the mean nodal signal intensity as a function of time and Figure 2*C* summarizes the mean difference between benign and malignant lymph nodes. As is evident, of all the time points evaluated, maximum contrast within lymph nodes was reached 24 hours after administration of nanoparticles and was 100% higher than during precontrast imaging.

Figure 3 is an example of a normal inguinal lymph node in a patient with prostate cancer. Serial imaging shows a time-dependent decrease of nodal signal intensity that reaches a maximum at 24 hours after administration. Note that the lymph node appears somewhat heterogeneous at 18 hours. Figure 4 is an example of a nonenlarged malignant perirectal

lymph node. Unlike in Figure 3, signal intensity changes are minor, indicative of malignancy.

A recent advance in automated nodal staging has been the development of automated segmentation, analysis, and visualization software [14]. To test whether these methods could be applied to ferumoxytol-based data sets, we chose to investigate benign and malignant examples. As is shown in Figure 5, semiautomated algorithms could be used to visualize the spatial location of individual nodes (and their status) in relations to pelvic vessels, bladder, prostate, and pelvis.

Discussion

Magnetic nanoparticles have become important tools for clinical cancer imaging [1,7,14]. A number of monocrystalline [15] and ultrasmall iron oxide [4] preparations have been developed over the last decade and have been shown to significantly improve the accuracy of nodal cancer staging [5,7,14,16]. They have also allowed steady-state angiogenesis imaging [17] and mapping of tumor host response (monocyte/macrophage phagocytosis) [18]. More recently, magnetofluorescent nanoparticles have been used experimentally for preoperative staging and intraoperative tumor localization [19]. Finally, molecularly targeted MNPs may enable high-resolution mapping of specific molecular targets and cellular components [20].

One of the most widely tested magnetic nanomaterials for *in vivo* imaging has been dextran-coated monocrystalline iron oxide. Recently, we confirmed earlier mouse model work [16] and showed that nanoparticle-enhanced MRI is vastly superior to other noninvasive methods of identifying lymph node metastases from solid tumors [7,14]. In addition, MRI can identify malignant lymph nodes outside the usual field of
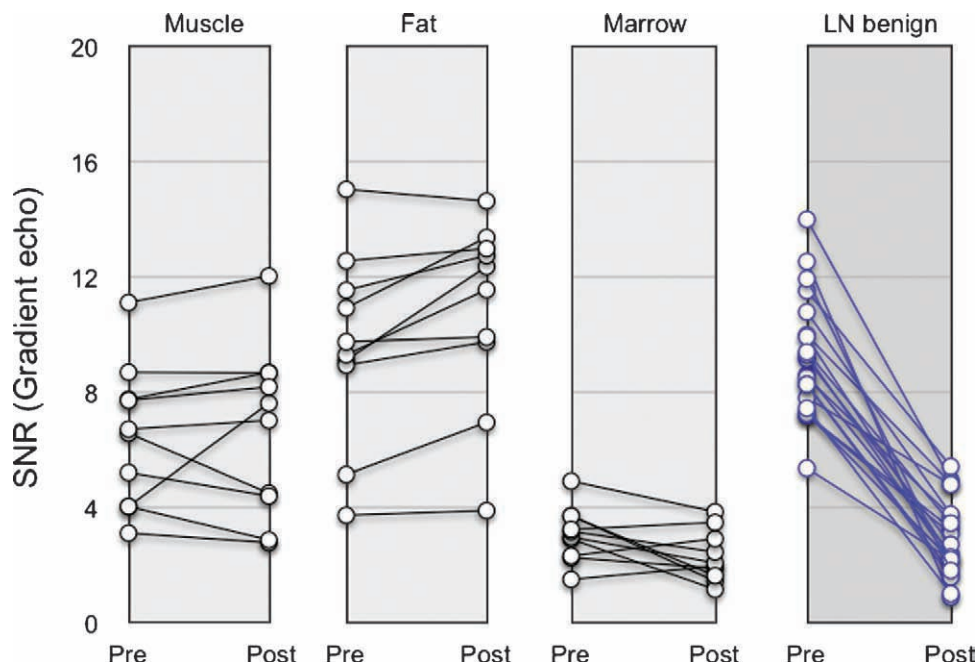

Figure 1. *Line graph showing SNR changes of normal tissue and lymph nodes before and 24 hours after administration of ferumoxytol (4 mg Fe/kg). Most tissues and malignant nodes show little or no change in SNR in comparison to benign lymph nodes.*
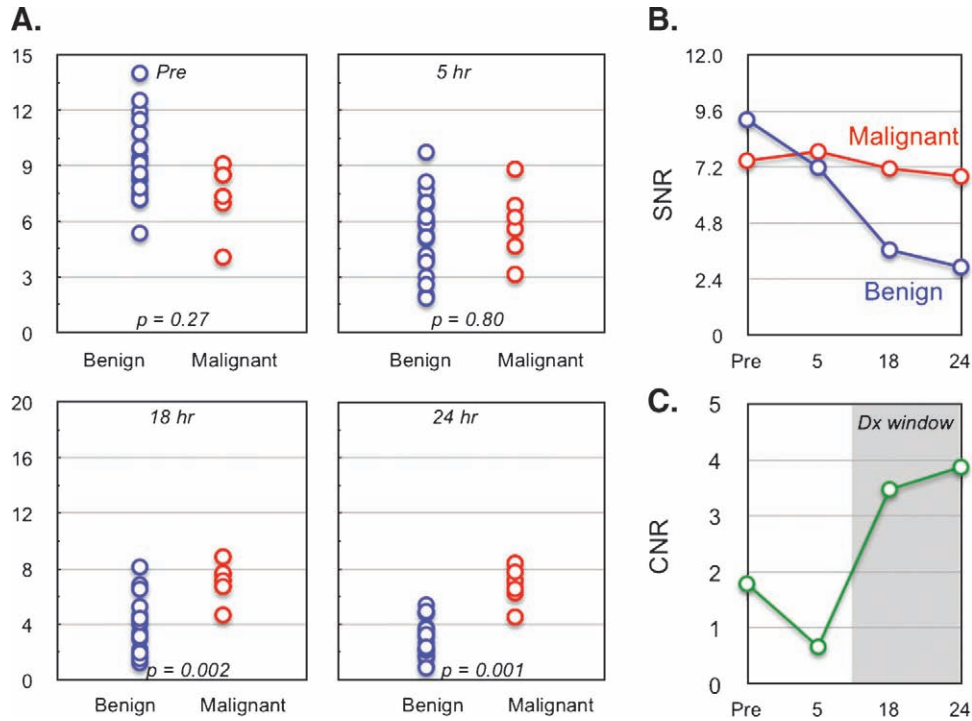
Figure 2. *(A) Scatter plot showing distribution of mean SNR values for benign and malignant node groups at different time points. P values reflect the statistical significance at different time points. (B) Line graph summarizing the mean change of malignant and benign nodal SNR over time. (C) Plot of CNR ratio between malignant and benign lymph nodes as a function of time. Note that overall contrast increases ~100% and that maximum CNR is reached at 24 hours.*

tumor resection, thus *upstaging* a proportion of cases that would have been classified as node-negative by conventional surgical staging. This method is useful for detecting loco-regional metastases that do not produce an overall increase in lymph node size and may be particularly valuable in clinical situations where surgical resection of all nodal tumor sites has been shown to improve cure rates (i.e., testicular and bladder cancer).
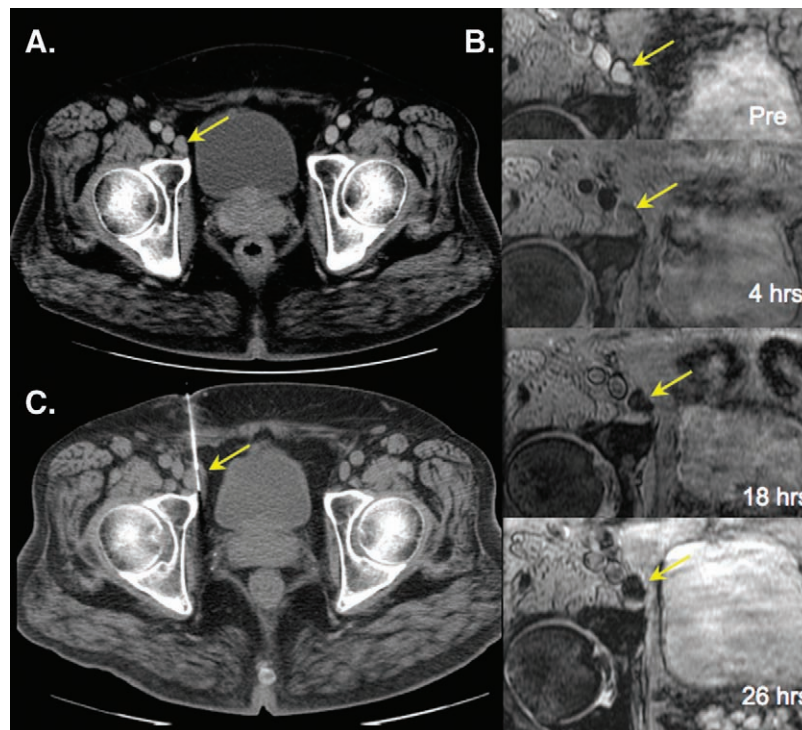

Figure 3. *Benign right external iliac node. (A) Axial contrast-enhanced computed tomographic (CT) image shows an enlarged right external iliac node. (B) Sequential images show progressive loss of signal following ferumoxytol administration. (C) CT-guided biopsy showing biopsy needle within the enlarged lymph node.*
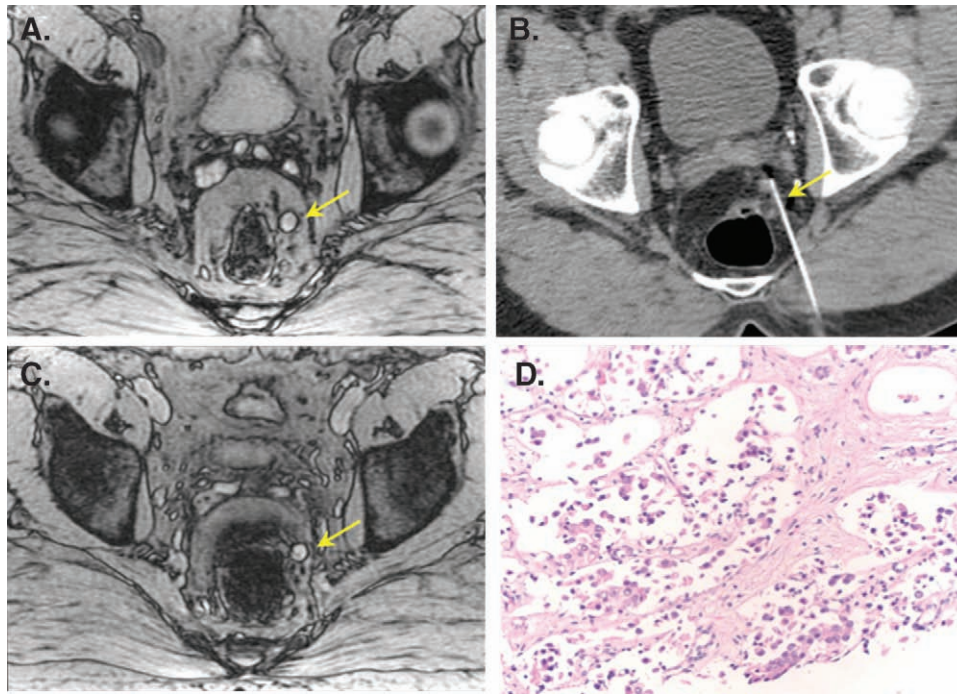
Figure 4. *Malignant left perirectal node. (A) Axial precontrast gradient-echo image shows a hyperintense left perirectal lymph node (arrow). (B) 24 hours after ferumoxytol, the node shows no signal change indicating malignant infiltration. (C) CT-guided biopsy of the node. (D) Subsequent pathologic evaluation showed architectural distortion from malignant infiltration of prostate cancer.*

The current preliminary study was designed to test whether an emerging, next-generation carboxymethyl dextran–based iron oxide nanoparticle (ferumoxytol) could be used to achieve similar results in nodal staging. Ferumoxytol was designed to minimize allergic reactions, such as those seen with commercially available iron dextran products, and to minimize free iron during dosing. By virtue of its different coating, ferumoxytol has a lower risk of immunogenicity, a better safety profile, and can be given by bolus administration [12,13]. However, it had also been reported to result in much more pronounced T1 shortening of blood and tissues, whereas its effects on nodal signal intensity (and hence its use for nodal staging)
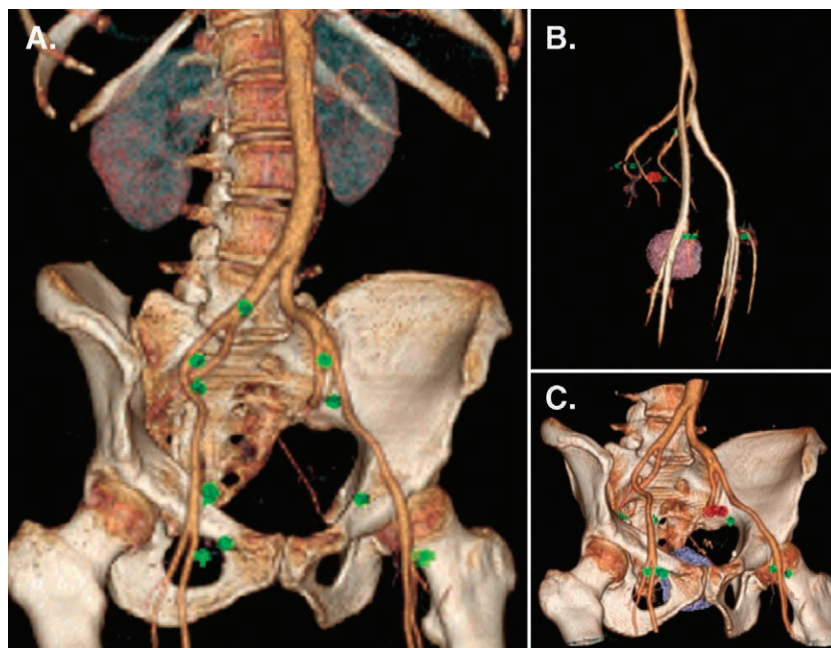

Figure 5. *Three-dimensional (3D) rendered images following IV administration of nanoparticles. (A) 3D rendered image from a patient shows multiple benign nodes (in green) plotted in relation to pelvic vessels and bony pelvis. (B) 3D rendered image of another patient shows malignant node (in red) in relationship to pelvic vasculature along with other benign nodes. (C) Same node in B is shown in relationship to pelvic vessels, bony pelvic, and the prostate gland.*

remained unknown. Our results indicate that ferumoxytol indeed alters nodal signal intensity on T2*-weighted MRI in a time-dependent fashion. Specifically, we show that the difference between normal and malignant nodes is highest 24 hours after administration. This preparation has the potential to become the next-generation lymphotrophic MR imaging agent.

We used a dose of 4 mg of Fe/kg, higher than the dose previously used in ferumoxtran clinical trials (2.6 mg Fe/kg). Despite the higher dose, the signal changes were less pronounced than those with ferumoxtran and the differentiation (delta contrast-to-noise [CNR]) was lower than with a lower dose of ferumoxtran. To increase the differential and further improve differentiation of benign and malignant nodes, we expect that higher doses will be ultimately required. Because higher doses of ferumoxytol can be given therapeutically (typically 1000 mg *vs* 280 mg as was the case for this diagnostic study) with few side effects, this distinct possibility exists and should be studied. It should also be noted that, as expected from the anemia studies, no side effects or adverse events were observed in the current study.

Improved noninvasive lymph node staging in cancer is critical to improving therapeutic outcomes by better selection of appropriate therapies for patients. In prostate cancer, for example, nodal involvement has been decreasing steadily because the advent of prostate-specific antigen (PSA) screening and earlier stage presentation. However, there has also been a trend toward more limited lymph node dissections, eliminating the external iliac dissection [21]. These smaller procedures may leave more patients with cancer in place postprostatectomy. More accurate preoperative nodal imaging will help select patients for larger lymph node dissections. Moreover, it may even eliminate the need for surgery at all, as the identification of malignant lymph nodes before radical prostatectomy often results in abandonment of a surgical approach in favor of castration therapy, potentially with radiation.

Magnetic nanoparticles have significant promise to improve lymph node staging. Our data indicate that ferumoxytol, a third-generation MNP, has potential as a lymph node staging agent with improved safety profiles and easier delivery. Moreover, we anticipate that this material may also have the potential to better delineate primary tumors, to map the vascular supply of primary tumors preoperatively, to image angiogenic changes associated with therapies, and to detect metastases to other organs. An approval for its anemia indication along with the feasibility data from this study will allow for our planned larger studies to evaluate incremental dosing, sensitivity, specificity, and ultimately the clinical value of this nanomaterial for cancer patients.

References

[1] Ferrari M (2005). Cancer nanotechnology: opportunities and challenges. *Nat Rev Cancer* **5**, 161–171.

[2] Fox JL (2000). Researchers discuss NIH's nanotechnology initiative. *Nat Biotechnol* **18**, 821.

[3] Guzman KA, Taylor MR, and Banfield JF (2006). Environmental risks of nanotechnology: National Nanotechnology Initiative funding, 2000–2004. *Environ Sci Technol* **40**, 1401–1407.

[4] Weissleder R, Elizondo G, Wittenberg J, Rabito CA, Bengele HH, and Josephson L (1990). Ultrasmall superparamagnetic iron oxide: characterization of a new class of contrast agents for MR imaging. *Radiology* **175**, 489–493.

[5] Weissleder R, Elizondo G, Wittenberg J, Lee AS, Josephson L, and Brady TJ (1990). Ultrasmall superparamagnetic iron oxide: an intravenous contrast agent for assessing lymph nodes with MR imaging. *Radiology* **175**, 494–498.

[6] Harisinghani MG, Saini S, Slater GJ, Schnall MD, and Rifkin MD (1997). MR imaging of pelvic lymph nodes in primary pelvic carcinoma with ultrasmall superparamagnetic iron oxide (Combidex): preliminary observations. *J Magn Reson Imaging* **7**, 161–163.

[7] Harisinghani MG, Barentsz J, Hahn PF, Deserno WM, Tabatabaei S, van de Kaa CH, de la Rosette J, and Weissleder R (2003). Noninvasive detection of clinically occult lymph-node metastases in prostate cancer. *N Engl J Med* **348**, 2491–2499.

[8] Anzai Y (2004). Superparamagnetic iron oxide nanoparticles: nodal metastases and beyond. *Top Magn Reson Imaging* **15**, 103–111.

[9] Bellin MF, Lebleu L, and Meric JB (2003). Evaluation of retroperitoneal and pelvic lymph node metastases with MRI and MR lymphangiography. *Abdom Imaging* **28**, 155–163.

[10] Bellin MF, Roy C, Kinkel K, Thoumas D, Zaim S, Vanel D, Tuchmann C, Richard F, Jacqmin D, Delcourt A, et al. (1998). Lymph node metastases: safety and effectiveness of MR imaging with ultrasmall superparamagnetic iron oxide particles—initial clinical experience. *Radiology* **207**, 799–808.

[11] Landry R, Jacobs PM, Davis R, Shenouda M, and Bolton WK (2005). Pharmacokinetic study of ferumoxytol: a new iron replacement therapy in normal subjects and hemodialysis patients. *Am J Nephrol* **25**, 400–410.

[12] Li W, Tutton S, Vu AT, Pierchala L, Li BS, Lewis JM, Prasad PV, and Edelman RR (2005). First-pass contrast–enhanced magnetic resonance angiography in humans using ferumoxytol, a novel ultrasmall superparamagnetic iron oxide (USPIO)–based blood pool agent. *J Magn Reson Imaging* **21**, 46–52.

[13] Spinowitz BS, Schwenk MH, Jacobs PM, Bolton WK, Kaplan MR, Charytan C, and Galler M (2005). The safety and efficacy of ferumoxytol therapy in anemic chronic kidney disease patients. *Kidney Int* **68**, 1801–1807.

[14] Harisinghani MG and Weissleder R (2004). Sensitive, noninvasive detection of lymph node metastases. *PLoS Med* **1**, e66.

[15] Shen T, Weissleder R, Papisov M, Bogdanov A Jr, and Brady TJ (1993). Monocrystalline iron oxide nanocompounds (MION): physicochemical properties. *Magn Reson Med* **29**, 599–604.

[16] Wunderbaldinger P, Josephson L, Bremer C, Moore A, and Weissleder R (2002). Detection of lymph node metastases by contrast-enhanced MRI in an experimental model. *Magn Reson Med* **47**, 292–297.

[17] Bremer C, Mustafa M, Bogdanov A Jr, Ntziachristos V, Petrovsky A, and Weissleder R (2003). Steady-state blood volume measurements in experimental tumors with different angiogenic burdens a study in mice. *Radiology* **226**, 214–220.

[18] Enochs WS, Harsh G, Hochberg F, and Weissleder R (1999). Improved delineation of human brain tumors on MR images using a long-circulating, superparamagnetic iron oxide agent. *J Magn Reson Imaging* **9**, 228–232.

[19] Josephson L, Kircher MF, Mahmood U, Tang Y, and Weissleder R (2002). Near-infrared fluorescent nanoparticles as combined MR/optical imaging probes. *Bioconjug Chem* **13**, 554–560.

[20] Weissleder R, Moore A, Mahmood U, Bhorade R, Benveniste H, Chiocca EA, and Basilion JP (2000). *In vivo* magnetic resonance imaging of transgene expression. *Nat Med* **6**, 351–355.

[21] Swanson GP, Thompson IM, and Basler J (2006). Treatment options in lymph node–positive prostate cancer. *Cancer* **106**, 2531–2539.